JOURNAL OF CATALYSIS 127, 595–604 (1991)

Stabilization of Alumina toward Thermal Sintering by Silicon Addition

BERNARD BEGUIN, EDOUARD GARBOWSKI, AND MICHEL PRIMET*

Institut de Recherches sur la Catalyse, Laboratoire Propre du CNRS, Conventionné à l'Université Claude Bernard Lyon I,2 Avenue Albert Einstein, 69626 Villeurbanne Cedex, France

Received March 8, 1990; revised July 16, 1990

The thermal stability of gamma alumina toward sintering at high temperatures (in the 1050–1220°C range) in the presence of steam has been studied from both structural and textural points of view. Improvement of the stabilization of alumina has been found be grafting silicon-containing compounds on the alumina surface. A reaction between the hydroxyl groups of alumina and the silicon-containing precursor was found to occur. The silicon-modified alumina is constituted by a layer of silica firmly bonded to the alumina support. The stabilization increases with increasing silicon loadings and reaches a plateau for ca. 3 wt% silicon.

INTRODUCTION

The catalytic combustion of hydrocarbons, especially methane, has received great attention for the regulation of emission pollutants. This process is particularly well adapted to the production of energy and heat in the field of drying. On the industrial scale, the catalysts presently used are based on noble metals (Pt, Pd, and Rh) deposited on alumina (*1*). Alumina in its gamma form is the most commonly used support. Alumina can be used alone or doped with colloidal silica in the form of fibrous material (*2*). Alumina can also be present as a washcoat of refractory materials of low specific area. Among these materials, fibers made of silica, based ceramic monoliths, and metallic monoliths are the most frequently found (*3, 4*).

During the operating conditions the catalysts are submitted to the action of water at elevated temperatures. The measure of the real temperature of the catalyst is a difficult task because of the presence of hot spots in the catalytic bed. In the vicinity of 1000°C and in the presence of water, the specific area of the gamma form of alumina strongly decreases (*5*): this sintering is associated with the transformation of alumina into the alpha phase. The thermal sintering of the support contributes to the deactivation of the catalyst because of the sintering of the noble metal particles and the encapsulation of the metallic phase by the support.

Numerous works have been devoted to the stabilization of alumina toward thermal sintering. Promoters have been introduced during the preparation of alumina or added by impregnation onto commercially available aluminas in order to improve the thermal stability of this support. Rare earth based promoters (*6*) have been extensively described in the patent literature with this objective. Among these promoters lanthanum in association with neodymium is certainly the most widely encountered and studied. Some more fundamental papers have proposed explanations for the stabilizing effect of adducts like lanthanum (*7–14*). Ceria is also used in conjunction with lanthanum, in the catalytic automotive converters, because of its specific properties toward oxygen storage (*15, 16*).

Alkaline-earth metal ions are also effective promoters for the stability of gamma

* To whom correspondence should be addressed.

0021-9517/91 $3.00

alumina toward thermal sintering. Specific areas as high as 10 $m^2 g^{-1}$ can be observed after aging at 1600°C for alumina doped with barium; the formation of barium hexaaluminate BaO, 6 Al_2O_3 could be at the origin of this stabilization (*17*).

Silicon was also found, in the patent literature, to be a good candidate for the stabilization of alumina (*18–21*). It can be introduced in the form of colloidal silica or of silicon-containing organometallic compounds. In the open literature, no fundamental study concerning the reasons for this improvement in the stability of alumina has been found. The aim of this paper is to measure the extent of the stabilizing effect of silicon, to study the state of the silicon deposited on alumina, and to propose an explanation for the positive effect of silicon.

EXPERIMENTAL

Materials

The starting material is an alumina supplied by Rhône-Poulenc (SCM 129). X-ray diffraction measurements showed the presence of the gamma and delta forms. The BET area of this support was found to be 107 $m^2 g^{-1}$, and the pore volume was close to 0.62 $cm^3 g^{-1}$.

Silicon was introduced using tetraethoxy silicon $Si(OC_2H_5)_4$ as precursor. A known amount of tetraethoxy silicon was dissolved in 200 ml of ethanol. Added to the previous solution was 50 g of SCM 129 alumina (50–125 μm granulometry). SCM 129 alumina was not pretreated prior to the modification. The mixture was maintained under stirring for 1 h at 60°C. Then ethanol was removed under reduced pressure using a rotary evaporator. The obtained solid was dried overnight at 110°C. In the final step, the material was treated under flowing oxygen (6 liters h^{-1}) at 500°C for 12 h with a slow heating rate (1°C min^{-1}). During the oxygen treatment, $Si(OC_2H_5)_4$ in excess was removed and the carbon-containing ligands were burned off.

Aging Test

Pure alumina as well as the silicon-modified aluminas were aged under a flow of air at elevated temperatures (1050 and 1220°C) in the presence or in the absence of a known amount of water (20 vol.%). This percentage corresponds to the amount of water formed during the combustion of a stoichiometric air + methane mixture. The weight of the sample was 3 g and the flow of effluents was close to 10 liters h^{-1}. Three aging tests were usually performed in the following conditions:

—at 1050°C for 24 h under dry air,

—at 1050°C for 24 h under air + 20 vol. % water,

—at 1220°C for 24 h under air + 20 vol. % water.

Physicochemical Measurements

BET areas were measured by nitrogen adsorption at −196°C. The cummulated pore volume was determined after recording the complete adsorption–desorption isotherm of nitrogen at the same temperature according to the Mikhail–Brunnauer–Bodor theory (*t* curve method).

The phase structure was determined by X-ray diffraction. A Siemens generator equipped with a back graphite monochromator was used. An average wavelength of 154.18 pm was taken for the Cu$K\alpha_1$–Cu$K\alpha_2$ radiation.

Transmission electron microscopy (TEM) measurements were performed on a JEOL 1200 EX instrument with a resolution of 0.2 nm. The samples were suspended in ethanol, a drop of the suspension was deposited on a carbon-coated copper grid, and ethanol was evaporated.

An infrared Fourier transform spectrometer (IFS 110 from Bruker) was used for the analysis of the hydroxyl groups present at the surface of the solids. Samples were pressed in order to obtain thin self-supported wafers of known weight. They were introduced in a cell allowing thermal treat-

TABLE 1

Specific Surface Area (S), Pore Volume (V_p), and Crystalline Phases of Starting SCM 129 Alumina after Aging Tests Performed in Various Conditions

Aging test		S ($m^2 g^{-1}$)	V_p ($cm^3 g^{-1}$)	XRD observed phases
Temp (°C)	$\%H_2O$			
500	0	107	0.62	$\gamma + \delta$
1050	0	57.4	0.11	$\theta + \alpha$
1050	20	26.4		$\theta + \alpha$
1220	20	4	0.007	Pure α

ments under controlled atmospheres (*22*). Spectra were recorded at room temperature with a resolution of 4 cm^{-1} and the number of scans was fixed to 100.

RESULTS AND DISCUSSION

Aging of the Starting Alumina

Table 1 shows the influence of the temperature as well as the effect of the presence of water on the specific area, the pore volume, and the XRD pattern of SCM 129 alumina. After 24 h of aging at 1220°C in the presence of 20 vol.% of water, alumina was transformed into its alpha form (Fig. 2A) with a dramatic decrease of the specific area (4 $m^2 g^{-1}$) and of the pore volume. As expected, the loss of specific area is more limited after an aging at 1050°C. Nevertheless, at 1050°C, Table 1 shows the effect of the presence of water during the sintering process of alumina. As mentioned in previous work (*5*), the introduction of water, at a given temperature, increases the loss of the specific area of oxide supports.

Aging of the Silicon-Modified Aluminas

Silicon-modified aluminas with silicon contents comprised between 0.91 and 3.16 wt% have been prepared according to the procedure described in the experimental part. In one impregnation step, the maximum amount of silicon remaining on the sample after calcination at 500°C corresponds to a loading close to 2.13 wt%. So the 3.16 wt% Si–Al_2O_3 was prepared from the 2.13 wt% Si one by treating this solid after the calcination under oxygen at 500°C by $Si(OC_2H_5)_4$ in ethanolic solution.

After calcination under oxygen at 500°C, the BET areas of the silicon-modified aluminas (Table 2) are close to the specific area of the starting alumina material. This behavior suggests that the introduction of silicon does not lead to a filling of the pores of alumina. According to the BET surface areas and silicon loadings, the coverage in silicon atoms comprised between 1.97 and 6.85 Si nm^{-2}. In addition, after the oxygen treatment at 500°C, X-ray patterns showed the presence of only delta alumina. In addition, no peak attributed to a silica phase was detected.

The main features of the silicon-containing samples after aging under the more severe conditions previously described were given in Table 2. The stability of alumina toward thermal sintering in the presence of water increases with the silicon content. Figure 1 shows the change of the BET area as a function of the silicon content for samples aged for 24 h at 1220°C in the presence of 20 vol.% of water. The stability of alumina increases with the silicon loading since the BET area of such samples follows the

TABLE 2

Specific Surface Area (S), Pore Volume (V_p), and Crystalline Phases of Silicon-Modified Aluminas after Aging Tests

Wt% Si	Temp (°C)	$\%H_2O$	S ($m^2 g^{-1}$)	V_p ($cm^3 g^{-1}$)	XRD observed phases
0.91 wt%	500	0	112	0.48	δ
1.97 Si/nm^2	1220	20	8	0.014	$\alpha + \theta$
1.35 wt%	500	0	111	0.55	δ
2.9 Si/nm^2	1220	20	30	0.18	$\alpha + \theta$
2.13 wt%	500	0	112	0.52	δ
4.6 Si/nm^2	1220	20	44	0.29	θ
3.16 wt%	500	0	111	0.45	δ
6.85 Si/nm^2 double grafting	1220	20	51	0.19	θ

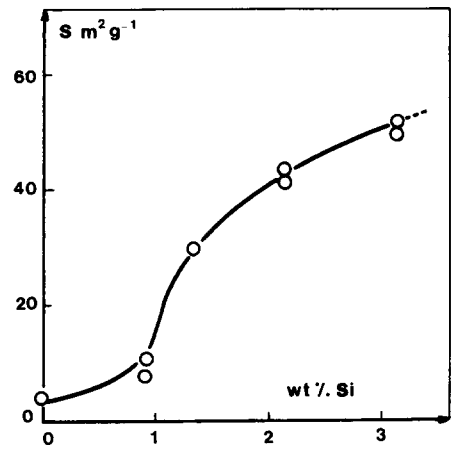

FIG. 1. Variation of the specific area of silicon-modified aluminas as a function of the silicon loading. Samples were aged for 24 h at 1220°C under an air + 20 vol.% water mixture.

amount of introduced silicon and then reaches a plateau for silicon loading exceeding 3 wt% Si, i.e., a density of 6.85 Si atoms per nm^2. By comparison with the highest surface OH-density of alumina, it appears that around half of the hydroxyl groups of Al_2O_3 are involved in the grafting of silicon. In the meantime, the proportion of alpha alumina in the sintered samples decreases when increasing the loading of silicon. For silicon contents corresponding to the plateau observed for the specific area, only the theta phase of alumina is detected in the X-ray diffraction diagram of the aged silicon-modified alumina (Fig. 2B). In addition, no diffraction peak typical of a crystalline form of silica has been observed, suggesting a strong interaction of the silicon adduct with the starting alumina material.

The same behavior was observed after an aging of the various samples at 1050°C under 20 vol.% of water; the stabilizing effect of silicon was even more pronounced. For instance, the silicon-modified alumina sample containing 3.16 wt% Si has a BET area of 88 $m^2 g^{-1}$ after such a sintering test instead of 26 $m^2 g^{-1}$ for the alumina sample free of silicon. The loss of specific area by comparison with the starting material does not exceed 20% after the aging test. In addition, in the aged sample, alpha alumina was not detected; the only identified phase was delta alumina (Fig. 3).

TEM measurements are in agreement with the high thermal stability of Si-containing alumina samples. The starting alumina sample exhibits sheets (400 nm × 100 nm) with pores of diameter close to 5 nm. After heating at 1220°C in the presence of water vapor, large particles of alpha alumina were detected (Fig. 4a). TEM micrographs of the fresh 3.16 wt% $Si-Al_2O_3$ sample are similar to those of the original SCM 129 alumina. In contrast, aging at 1220°C in the presence of

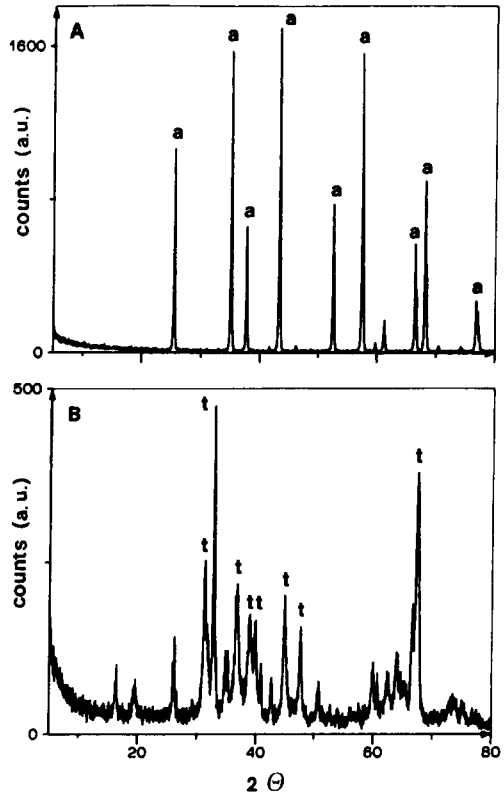

FIG. 2. X-ray diffraction patterns of pure alumina (A) and silicon-modified alumina (3.16 wt% Si) (B) after aging for 24 h at 1220°C under an air + 20 vol.% water mixture. An average wavelength of 154.18 pm was used for the $CuK\alpha_1$–$CuK\alpha_2$ radiation: Peaks labeled "a" are due to the alpha alumina phase; peaks labeled "t" are due to the theta alumina phase.

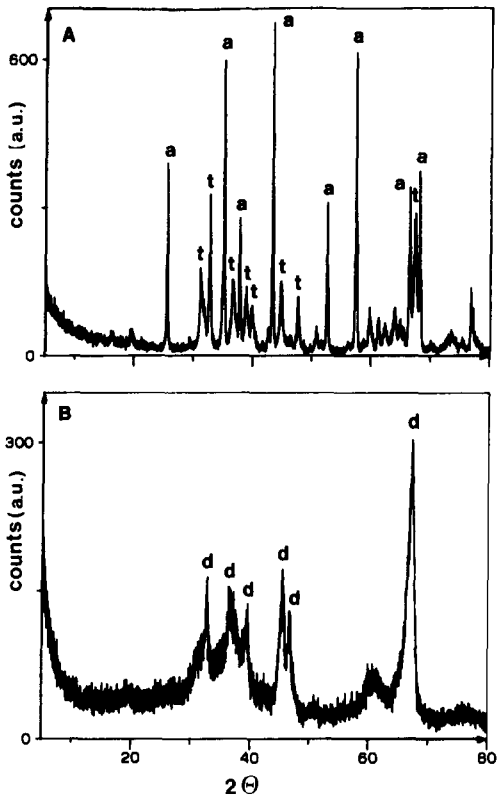

FIG. 3. X-ray diffraction patterns of pure alumina (A) and silicon-modified alumina (3.16 wt% Si) (B) after aging for 24 h at 1050°C under an air + 20 vol.% water mixture. An average wavelength of 154.18 pm was used for the Cu$K\alpha_1$–Cu$K\alpha_2$ radiation: Peaks labeled "a" are due to the alpha alumina phase; peaks labeled "t" are due to the theta alumina phase; peaks labeled "d" are due to the delta alumina phase.

water does not deeply change the size of the sheets. Moreover, the aged sample shows the presence of needles instead of large alpha alumina particles (Fig. 4b).

Surface Hydroxyl Groups

Alumina and silicon-modified aluminas were first calcined under oxygen at 500°C in a reactor. After cooling down to room temperature, the samples were compressed in order to obtain a wafer which was introduced into the infrared cell (*22*). The pellets were treated again under a flow of oxygen at 500°C and evacuated at the same temperature. After such a treatment, the infrared spectrum of the SCM 129 alumina exhibits four main ν OH bands located at 3760 cm^{-1} (weak), 3730 cm^{-1} (strong), 3685 cm^{-1} (medium), and 3580 cm^{-1} (broad) (Fig. 5a).

The nature of the hydroxyl groups of alumina has been extensively studied by infrared spectroscopy. For highly dehydroxylated alumina surfaces, the ν OH bands observed have been assigned to hydroxyl groups linked either to aluminum ions having various environments of oxygen ions (*23*) or to aluminum ions in octahedral or tetrahedral symmetry (*24*). The alumina sample in the present study was dehydroxylated at lower temperature, i.e., 500°C in comparison with similar solids examined in the works of Peri (*23*) and Knözinger and Ratnasamy (*24*). As a consequence, the hydroxyl groups are not isolated and bands at lower wavenumbers, for instance, the bands at 3685 and 3580 cm^{-1}, are observed at the expense of the bands due to the isolated hydroxyl groups.

The introduction of increasing amounts of silicon on the starting material (SCM 129 sample) leads to the following features (Figs. 5a–5e):

(i) the formation of a ν OH band at 3745 cm^{-1}; its intensity increased with the amount of introduced silicon,

(ii) the intensities of the bands of hydroxyl groups attributed to the alumina were strongly reduced by increasing the silicon loadings; they were absent in the spectrum of the more loaded silicon sample (3.16 wt% Si) (Fig. 5e).

The appearance and the growth in intensity of the 3745-cm^{-1} band associated with the increase of silicon content must be connected with the formation of increasing amounts of silanol groups at the surface of the sample. In fact, previous infrared spectroscopic studies of pure silica have shown the presence of two types of OH species (*25*):

—isolated and surface hydroxyl groups

detected by a sharp ν OH band at ca. 3740–3750 cm^{-1},

—internal or hydrogen bonded hydroxyl groups exhibiting a broad ν OH band close to 3550 cm^{-1}.

According to the previous assignments, the infrared spectrum of the 3.16 wt% Si–Al_2O_3 sample presents only two ν OH bands at 3745 and 3575 cm^{-1} which can be reasonably attributed to hydroxyl groups of a silica layer bonded to a sublayer of alumina.

The optical densities of the ν OH bands can be expressed per gram of catalyst with the knowledge of the weight of the wafer. Figure 6 shows the change of the intensity of the 3745 cm^{-1} band as a function of the silicon content: the optical density of this band increases continuously and almost linearly with the amount of silicon, suggesting a homogeneous distribution of silanol groups and of silica of the surface of alumina. The intensity of the 3745 cm^{-1} band is not equal to zero for pure alumina since the starting material exhibits a ν OH band at 3730 cm^{-1}, very close to the band due to free silanol groups.

The coverage of the alumina surface by silica can also be monitored by the change of the ratio of the absorbance of the 3745-cm^{-1} band to the absorbance of the 3680-cm^{-1} band. In the conditions of desorption used in the present study, the 3680-cm^{-1} band appears typical of the alumina surface whereas both alumina and silica contribute to the 3745-cm^{-1} band. Figure 7 shows the change of the β ratio (where β = OD 3685-cm^{-1} band/OD 3745-cm^{-1} band) as a function of the silicon content. The β ratio decreases with increasing amounts of introduced silicon showing, as in the preceding case, a progressive coverage of the alumina surface by silica.

Since the introduction of silicon is accompanied by a decrease of the intensity of the ν (OH) bands of alumina, an interaction of the $Si(OC_2H_5)_4$ precursor with the hydroxyl groups of alumina may be postulated according to the scheme

$$\text{—Al—OH} + Si(OC_2H_5)_4 \rightarrow \text{—Al—O—Si}(OC_2H_5)_3 + C_2H_5OH$$

During the treatment of the obtained sample at 500°C under flowing oxygen, the hydrocarbon chains are likely to be oxidized and hydroxyl groups bonded onto silicon are formed:

$$\text{—Al—O—Si}(OC_2H_5)_3 \xrightarrow{\text{(under } O_2 \text{ at 500°C)}} \text{—Al—O—Si}(OH)_3 + 6\ CO_2$$

Such a scheme has already been postulated for the chemical vapor deposition of silicon alkoxides on various oxide substrates (*26–29*).

The Si–OH groups so obtained are able to condense with other hydroxyl groups (linked to Si or Al atoms) in order to firmly anchor the silicon-containing layer to the alumina surface. Because of the size of the tetraethoxysilicon precursor, a full coverage of the alumina surface by $Si(OC_2H_5)_4$ cannot be reached in one step. The maximum loading obtained after a single impregnation corresponds to a silicon content of ca. 2.13 wt% Si, i.e., a coverage of 4.6 Si nm^{-2}. After an oxygen treatment at 500°C, some hydroxyl groups of alumina are now accessible to the silicon precursor allowing the grafting of larger amounts of silicon.

A Possible Role of Silicon in the Stabilization of Transition Aluminas

The thermal sintering of transition aluminas has been much studied, and in particular

FIG. 4. TEM micrographs of samples aged for 24 h at 1220°C under an air + 20 vol.% water mixture: (a) pure alumina; (b) silicon-modified alumina (3.16 wt% Si).

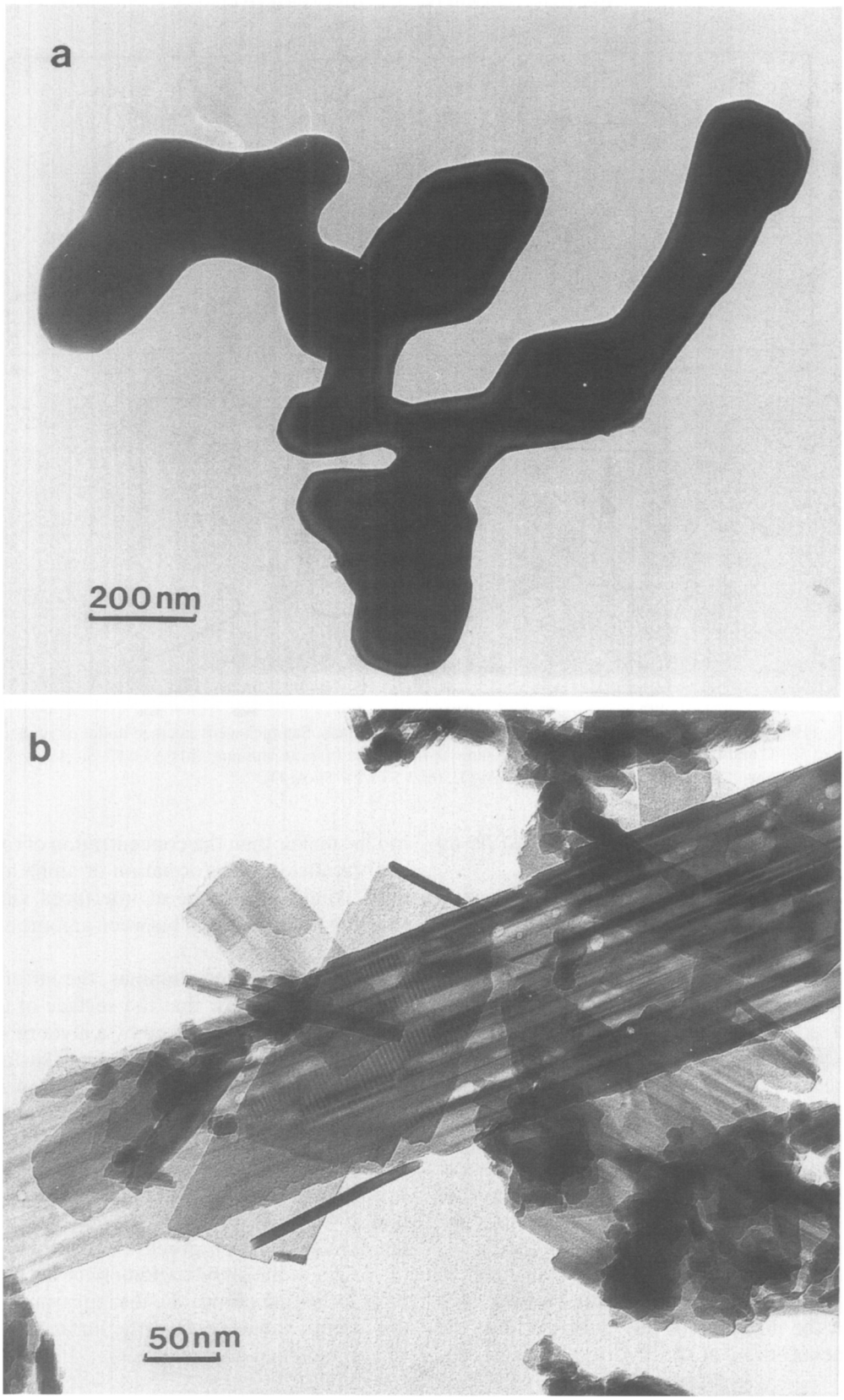
a
200nm
b
50nm

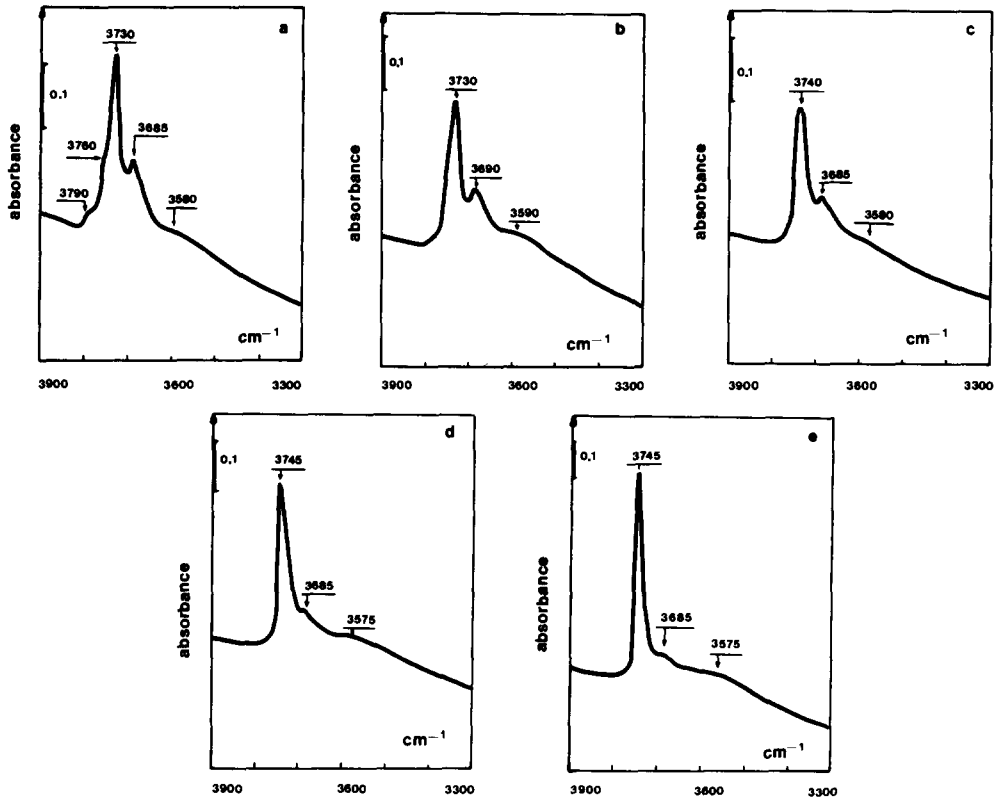

FIG. 5. Infrared spectra of pure and silicon-modified aluminas. Samples were calcined under oxygen at 500°C and treated under vacuum at the same temperature: (a) pure alumina; (b) 0.91 wt% Si–Al_2O_3; (c) 1.35 wt% Si–Al_2O_3; (d) 2.13 wt% Si–Al_2O_3; (e) 3.16 wt% Si–Al_2O_3.

the presence of water was found to be an accelerating factor (*1, 5*).

A mechanistic model for the sintering of anatase and alumina has been recently proposed (*30–34*); it takes into account the influence of water, the presence of hydroxyl groups, as well as the presence of cationic and anionic vacancies. The first step proposed in this model supposes a dissociative adsorption of water onto an anionic vacancy. In the following steps cation diffusion is postulated to occur by successive cycles of desorption–adsorption of water (*34*). The initial sintering by the transport of "AlO" building units was taken into account by this model. In addition, the rate of sintering was found to be proportional to $(P_{H_2O})^{0.5}$. However, the rate-limiting step was the diffusion of the hydroxyl ions; the concentration of the hydroxyl groups was much smaller than the concentration of oxygen vacancies. The formation of alpha alumina would take place at interfaces via a reaction of annihilation between anionic and cationic vacancies (*31*).

In silicon-modified aluminas, the infrared measurements show that the surface of the starting material is covered by a layer of silica; in such a case, the solid exhibits a surface silica behavior. Since the stabilization increases with the silicon coverage, one can assume that the surface species responsible for the sintering process are not present at the surface of the modified aluminas. The formation of Si–O–Si or Si–O–Al bridges during the dehydroxylation process is certainly at the origin of the stabilization effect because their formation allows the disappearance of the cationic vacancies from the surface of the silicon-modified aluminas.

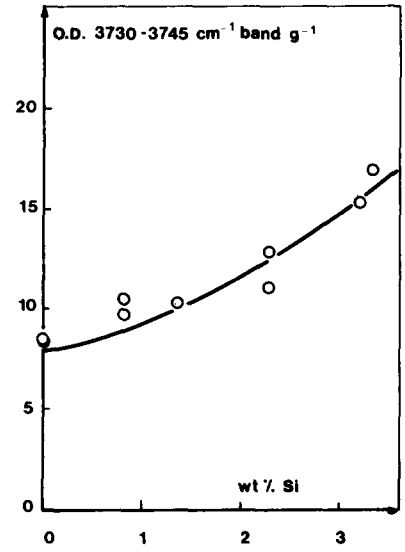

FIG. 6. Variation of the optical density (OD) of the (3730–3745 cm^{-1}) band as a function of the silicon content. OD was expressed per gram of catalyst and the samples were treated under oxygen then *in vacuo* at 500°C.

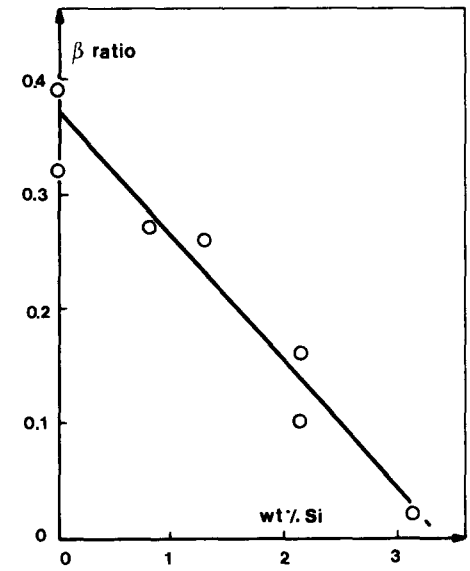

FIG. 7. Change of the β ration (OD 3685-cm^{-1} band/ OD 3730–3745-cm^{-1} band) as a function of the silicon content for samples treated under oxygen, then *in vacuo* at 500°C.

CONCLUSION

By contacting a gamma alumina with an ethanolic solution of $Si(OC_2H_5)_4$ a reaction occurs between the hydroxyl groups of Al_2O_3 and the silicon-containing compound. After calcination under oxygen, the surface exhibits silanol groups which develop at the expense of the hydroxyl groups of alumina. The stability of these solids toward thermal sintering in the presence of water vapor was improved in comparison with pure alumina. The stabilization increases with the silicon content. According to a model recently proposed to describe the sintering of alumina, it seems that the silica layer grafted to alumina is able to fill the anionic vacancies of alumina responsible for the thermal sintering in the presence of water.

ACKNOWLEDGMENTS

Financial support for this work has been provided by Gaz de France (Direction des Etudes et Techniques Nouvelles, Centre des Etudes et Recherches sur les Utilisations du Gaz). The authors fully acknowledge Mrs. M. T. Jimenez for X-ray diffraction measurements and Mr. J. Billy for infrared experiments.

REFERENCES

1. Trimm, D. L., *Appl. Catal.* **7,** 249 (1983).
2. Symes, W. R., and Rastetter, E., 24th International Colloquium on Refractories, Aachen, W. Germany, September 1981"; Murrell, L. L., Dispenziere, N. C., and Kim, K. S., *Catal. Lett.* **2,** 263 (1989).
3. Dwyer, F. G., *Catal. Rev. Sci. Eng.* **6,** 261 (1972).
4. Pfefferle, L. D., and Pfefferle, W. C., *Catal. Rev. Sci. Eng.* **29,** 219 (1987).
5. Harris, D. J., Young, D. J., and Trimm, D. L., *in* "Proceedings, 10th Australian Chemical Engineering Conference, 1982," p. 175 Sydney, August 1982.
6. Sauvion, G. N., and Ducros, P., *J. Less-Common Met.* **111,** 23 (1985).
7. Matsuda, S., Kato, A., Mizumoto, M., and H. Yamashita, *in* "Proceedings, 8th International Congress on Catalysis, Berlin, 1984," Vol. IV, p. 879. Verlag Chemie, Weinheim, 1984.
8. Oudet, F., Bordes, E., Courtine, P., Maxant, G., Lambert, C., and Guerlet, J. P., *in* "Catalysis and Automotive Pollution Control" (A. Crucq and A. Frennet, Eds.), p. 313. Elsevier, Amsterdam, 1987.
9. Oudet, F., Courtine, P., and Vejux, A., *J. Catal.* **114,** 112 (1988).
10. Oudet, F., Vejux, A., and Courtine, P., *Appl. Catal.* **50,** 79 (1989).
11. Schaper, H., Doesburg, E. B. M., and van Reijen, L. L., *Appl. Catal.* **7,** 211 (1983).

12. Schaper, H., PhD thesis, Delft University, 1984.
13. Schaper, H., Amesz, D. J., Doesburg, E. B. M., and van Reijen, L. L., *Appl. Catal.* **9,** 129 (1984).
14. Bettman, M., Chase, R. E., Otto, K., and Weber, W. H., *J. Catal.* **117,** 447 (1989).
15. Yao, H. C., and Yao, Y. F. Yu, *J. Catal.* **86,** 254 (1984).
16. Gauguin, R., Graulier, M., and Papee, D., *Adv. Chem. Ser.* **143,** 147 (1975).
17. Machida, M., Eguchi, K., and Arai, H., *J. Catal.* **103,** 385 (1987); Machida, M., Eguchi, K., and Arai, H. *Chem. Lett. Chem. Soc. Japan,* 151 (1986).
18. French Patent N°7,435,462.
19. British Patent N°1,492,274.
20. European Patent N°86,300,630.0
21. European Patent N°85,402,353.8.
22. Primet, M., Vedrine, J. C., and Naccache, C., *J. Mol. Catal.* **4,** 411 (1978).
23. Peri, J. B., *J. Phys. Chem.* **69,** 211 and 220 (1965).
24. Knözinger, H., and Ratnasamy, P., *Catal. Rev. Sci. Eng.* **17,** 31 (1978).
25. Kiselev, A. V., and Lygin, V. I., "Infrared Spectra of Surface Compounds" (English translation), Chap. IV. Wiley, New York, 1975.
26. Okuhara, T., and White, J. M., *Appl. Surf. Sci.* **29,** 223 (1987).
27. Sato, S., Toita, M., Yu, Y. Q., Sodesawa, T., and Nozaki, F., *Chem. Lett. Chem. Soc. Japan,* 1535 (1987).
28. Niwa, M., Hibino, T., Murata, H., Katada, N., and Murakami, Y., *J. Chem. Soc. Chem. Commun.,* 289 (1989).
29. Imizu, Y., and Tada, A., *Chem. Lett. Chem. Soc. Japan,* 1793 (1989).
30. Burtin, P., Brunelle, J. P., Pijolat, M., and Soustelle, M., *Appl. Catal.* **34,** 225 (1987).
31. Burtin, P., Brunelle, J. P., Pijolat, M., and Soustelle, M., *Appl. Catal.* **34,** 239 (1987).
32. Burtin, P., PhD thesis, Ecole Nationale Supérieure des Mines de Saint-Etienne, France, 1985.
33. Dauzat, M., PhD thesis, Ecole Nationale Supérieure des Mines de Saint-Etienne, France, 1989.
34. Pijolat, M., and Soustelle, M., *in* "VIIth World Round Table Conference on Sintering, 1989, Herug-Novi, Yugoslavia."